Published in final edited form as:
Neuroimage. 2014 February 15; 87: 32–41. doi:10.1016/j.neuroimage.2013.10.053.

Ultrashort Echo Time (UTE) Magnetic Resonance Imaging of the Short T2 Components in White Matter of the Brain Using a Clinical 3T Scanner

Jiang Du, PhD[1], **Guolin Ma, MD**[1,2], **Shihong Li, MS**[1], **Michael Carl, PhD**[3], **Nikolaus M Szeverenyi, PhD**[1], **Scott VandenBerg, MD, PhD**[4], **Jody Corey-Bloom, MD, PhD**[5], and **Graeme M Bydder, MB. ChB**[1]

[1]Department of Radiology, University of California, San Diego

[2]Department of Radiology, China-Japan Friendship Hospital, Beijing, China

[3]Global Applied Science Laboratory, GE Healthcare, San Diego

[4]Department of Pathology, University of California, San Diego

[5]Department of Neurosciences, University of California, San Diego

Abstract

White matter of the brain contains a majority of long T2 components as well as a minority of short T2 components. These are not detectable using clinical magnetic resonance imaging (MRI) sequences with conventional echo times (TEs). In this study we used ultrashort echo time (UTE) sequences to investigate the ultrashort T2 components in white matter of the brain and quantify their T2*s and relative proton densities (RPDs) (relative to water with a proton density of 100%) using a clinical whole body 3T scanner. An adiabatic inversion recovery prepared dual echo UTE (IR-dUTE) sequence was used for morphological imaging of the ultrashort T2 components in white matter. IR-dUTE acquisitions at a constant TR of 1000 ms and a series of TIs were performed to determine the optimal TI which corresponded to the minimum signal to noise ratio (SNR) in white matter of the brain on the second echo image. T2*s of the ultrashort T2 components were quantified using mono-exponential decay fitting of the IR-dUTE signal at a series of TEs. RPD was quantified by comparing IR-dUTE signal of the ultrashort T2 components with that of a rubber phantom. Nine healthy volunteers were studied. The IR-dUTE sequence provided excellent image contrast for the ultrashort T2 components in white matter of the brain with a mean signal to noise ratio of 18.7 ± 3.7 and a contrast to noise ratio of 14.6 ± 2.4 between the ultrashort T2 white matter and gray matter in a 4.4 min scan time with a nominal voxel size of 1.25×1.25×5.0 mm^3. On average a T2* value of 0.42 ± 0.08 ms and a RPD of 4.05 ± 0.88% were

Corresponding Address: Jiang Du, jiangdu@ucsd.edu, University of California, San Diego, Department of Radiology, 200 West Arbor Drive, San Diego, CA 92103-8756, Phone (619) 543-3512, Fax (619) 543-3736.

demonstrated for the ultrashort T2 components in white matter of the brain of healthy volunteers at 3T.

Keywords

Ultrashort echo time; adiabatic IR; ultrashort T2; white matter; T2*; proton density

Introduction

Myelin is a lamellar membranous structure consisting of alternating protein and lipid layers with approximately 20% protein and 80% lipid (van der Knaap MS and Valk J, 2005). It accounts for about 14% of the wet mass and 50% of the dry mass of white matter of the brain (van der Knaap MS and Valk J, 2005). Myelin is present in the form of the myelin sheath, which surrounds the axons of some neurons. It insulates the axons from electrically charged atoms and molecules and helps to increase nerve conduction velocity. Loss of the myelin sheath is the hallmark of numerous inflammatory and neurodegenerative disorders, including multiple sclerosis (MS) and different forms of leukodystrophy (van der Knaap MS and Valk J, 2005).

Imaging of myelin has been of central importance for both clinical and basic research studies in neuroradiology. Researchers have been working for decades to develop magnetic resonance imaging (MRI) techniques to accurately measure myelin in vivo (Stanisz GJ, et al, 1999; Whittall KP, et al, 1997; Wolff SD and Balaban RS, 1989). The non-water protons in myelin as well as protons in water tightly bound to myelin have very short T2s and are “invisible” when conventional clinical MR sequences are used (Horch RA, et al., 2011; Ramani A, et al, 2002). Two types of MR techniques have been developed to indirectly image myelin using the water associated with it. The first approach is based on a non-negative least-squares (NNLS) fit of T2 relaxation times using a 3-pool model consisting of myelin water (water trapped in the myelin sheath), axon water (water within myelinated axons) and mixed water (interstitial water) (Lancaster JL, et al., 2003; Whittall KP and MacKay AL, 1989). The myelin water fraction (MWF), defined as the ratio of the signal intensity of the shortest T2 component to the total, is used as an indirect measure of myelin content. The other approach employs magnetization transfer (MT), which exploits cross relaxation between myelin protons and tissue water to indirectly access myelin (Henkelman RM, et al, 2001; Ramani A, et al, 2002; Wolff SD and Balaban RS, 1989).

We have implemented a two-dimensional (2D) ultrashort echo time (UTE) sequence with a minimal nominal TE of 8 μs, giving it the potential to directly detect signal from myelin as well as water tightly bound to it (i.e., the ultrashort T2* components) in white matter of the brain. The purpose of the present study was to investigate the use of this technique in combination with suppression of long T2 components in white matter with an adiabatic inversion recovery preparation and dual echo UTE acquisition (2D IR-dUTE). This approach was used for direct imaging of the ultrashort T2* components and quantitative evaluation of T2* and relative proton density (RPD) in the white matter of healthy volunteers.

Methods

Pulse Sequence

Figure 1A shows the basic 2D UTE sequence which was implemented on a 3T Signa TwinSpeed scanner (GE Healthcare Technologies, Milwaukee, WI) which had a maximum gradient performance of 40 mT/m and 150 mT/m/ms. The sequence employed a half-pulse radiofrequency (RF) excitation (pulse duration = 472 μs, pulse bandwidth = 2.7 kHz) with the peak RF power deposited during the ramp down part of the slice selection gradient. The combination of variable rate selective excitation (VERSE), radial ramp sampling and fast transmit/receive switching allowed delay times (nominal TEs) as short as 8 μs between the end of the RF excitation and the beginning of the free induction decay (FID) data acquisition (Biswas R, et al, 2012; Du J, et al, 2007). A complete slice profile was generated by collecting data with the slice selection gradient in one polarity and adding this to data collected with the slice selection gradient polarity reversed. The half projections were repeated through 360° to cover the whole of k-space.

The conventional slice-selective 2D UTE sequence is subject to eddy currents which tend to distort the slice selection gradient resulting in out-of-slice signal excitation and inaccurate T2* measurement (Lu A, et al., 2008). A 2D non-slice selective UTE sequence was implemented by employing a short rectangular pulse (duration = 32 μs) for signal excitation, thus eliminating errors due to eddy currents associated with conventional half-pulse excitation. This sequence was expected to provide accurate measurement of T2* for ultrashort T2 species.

Contrast Mechanisms

The ultrashort T2* components only represent a small fraction of the total signal from white matter of the brain. The dominant signal is from the long T2 components. The surrounding gray matter as well as fat and CSF also produce much higher signals than the ultrashort T2* components in white matter of the brain. It is necessary to suppress these long T2 signals in order to generate contrast for the ultrashort T2* components (Du J, et al, 2010). Furthermore, the dynamic range can be maximized by efficient suppression of the long T2 signals in order to optimize the conspicuity of the ultrashort T2* components in white matter of the brain (Waldman A, et al, 2003). Figurer 1B shows the 2D IR-dUTE contrast mechanism. In this approach, an adiabatic fast passage (Silver-Hoult) inversion pulse (duration = 8.64 ms) is used to invert the longitudinal magnetization, including that of gray matter, fat, and CSF as well as the long T2 components in white matter. The longitudinal magnetization of the ultrashort T2* components is reduced but not inverted due to significant transverse relaxation during the long adiabatic inversion process (Larson PE, et al, 2007). UTE data acquisition starts at a delay time (TI) necessary for the inverted longitudinal magnetization of long T2 white matter to reach its null point. Assuming the same T1 for different long T2 components in white matter (Whittall KP, et al, 1997), uniform and complete suppression of long T2 white matter is anticipated. Other long T2 tissues such as the gray matter, CSF and fat have T1s that differ from that of long T2 white matter, and are inverted, but only partially nulled by the adiabatic IR pulse. Simulations based on the Bloch equations suggest that more than 90% of the long T2 signals from gray

matter and CSF are suppressed. The 2nd echo acquires signals from the residual long T2 tissues. There is zero or near zero signal from the ultrashort T2* components. Subtraction of the 2nd echo from the first one provides selective depiction of the ultrashort T2* components in white matter.

T2* Measurement

The approach to measurement of T2* is similar to the conventional strategy of varying TE while keeping TR constant. In order to monitor the ultrashort T2* components in white mater of the brain, however, the range of echo times needs to be significantly shorter than those used with conventional clinical MR imaging. Since signal from the ultrashort T2* components in white matter are far lower than those from the long T2 components in white matter as well as these from gray matter, fat and CSF, IR-dUTE images were acquired at a series of TE delays to selectively image and quantify T2* of the ultrashort T2* components using the following single exponential signal decay model:

$$S(TE)=S_0 \times e^{-TE/T2*}+C \quad [1]$$

where C accounts for the background noise, including pseudo-noise associated with undersampled IR-dUTE data acquisitions.

Relative Proton Density (RPD) Measurement

Similar to the assessment of bone water content, accurate estimation of proton density of the ultrashort T2* components requires consideration of relaxation and coil sensitivity effects. RPD can be calculated by comparing the IR-dUTE signal intensity of the ultrashort T2 components with that of a reference phantom. With IR-dUTE imaging, the short T2 magnetization is partially inverted by the long adiabatic inversion pulse, and then partly excited by the half RF pulse (Du J, et al, 2010; Techawiboonwong A, et al, 2008). The longitudinal magnetization μ_z(T2) after the adiabatic IR pulse, neglecting T1, is approximately (Du J, et al, 2010):

$$\mu_z(T2) \approx \mu_0 \times (1-T2 \times \int_{-\infty}^{\infty} \omega_1(t)^2 dt)=\mu_0 \times (1-P)=\mu_0 \times Q \quad [2]$$

P is the attenuation factor due to long adiabatic IR pulse. Introducing Q = 1−P, we can calculate relative proton densities using the following equation (Du J, et al, 2010):

$$RPD=\frac{I}{I_{ref}} \times \frac{f_{xy}^{ref}}{f_{xy}} \times \frac{1+(Q_{ref}-1)e^{-TI/T_{1,ref}})-Q_{ref}e^{-TR/T_{1,ref}})}{1+(Q-1)e^{-TI/T_1})-Qe^{-TR/T_1})} \times \frac{1-Qf_z \times e^{-TR/T_1})}{1-Q_{ref}\, f_z^{ref} \times e^{-TR/T_{1,ref}}} \times \frac{e^{-TE/T_{2,ref}}}{e^{-TE/T_2}} \times \frac{\eta_{ref}}{\eta} \times RPD_{ref} \quad [3]$$

where RPD and RPD_{ref} are the relative proton densities of the ultrashort T2* components and reference phantom, respectively. I and I_{ref} are the corresponding image intensities, η and η_{ref} are the corresponding coil sensitivities, f_{xy} and f_z describe the behavior of the transverse magnetization and longitudinal magnetization, respectively, as a function of the half pulse

profile as well as T2* and T1. Q, f_{xy} and f_z can be derived from Bloch equation simulation once T1 and T2* are known (Du J, et al., 2010).

In this study the external reference was a piece of rubber which has a short T2* of ~340 μs and a T1 of ~280 ms. According to the study of Nayak et al, the ultrashort T2 components in white matter of fixed brain have T2*s in the range of 100–350 μs (mean T2* ~ 200 μs) and T1s in the range of 200~500 ms (mean T1 ~ 350 ms). Both T1 and T2* of rubber are similar to those of the ultrashort T2 components in white matter of the brain. This minimizes errors associated with short T2 excitation and blurring. The rubber phantom was placed close to the human head. Variation in coil sensitivity was corrected by dividing the 2D IR-dUTE signal from white matter or rubber by the 2D UTE signal obtained from a separate scan of a bottle of water, which was large enough to cover the region occupied by both the human head and the rubber.

RPD of the rubber phantom was measured by comparing the 3D UTE signal of the rubber with that of a deuterium water (D_2O) and regular water (D_2O-H_2O) phantom consisting of seven different concentrations of H_2O (10%, 20%, 30%, 40%, 60%, 80% and 100%) mixed with ~20 mM $MnCl_2$. The 3D UTE sequence employed a short rectangular pulse (duration = 32 μs) excitation followed by 3D radial ramp sampling with a minimal nominal TE of 8 μs. The pulse duration is far shorter than the T2* of the rubber phantom and D_2O-H_2O phantoms, eliminating both T1 and T2* effects during excitation. A relatively long TR of 300 ms and a low flip angle of 10° were used to allow virtually full recovery of the longitudinal magnetization of rubber and D_2O-H_2O phantoms. Other imaging parameters included: FOV = 8 cm, 40000 projections, TE = 8 μs, BW = 125 kHz, reconstruction matrix size = 128×128×128, NEX = 1, scan time = 3.3 hours. A calibration curve (UTE signal vs. H_2O%) was generated from the D_2O-H_2O phantoms, and linear interpolation was used to calculate proton density in the rubber eraser.

Imaging Experiments

In total nine healthy volunteers (all male, age from 34 to 69 years, average age of 50 ± 14 years) were recruited for this study. Written informed consent approved by the Institutional Review Board was obtained prior to their participation. An eight-channel head coil was used for signal reception and the body coil was used for excitation.

The IR-dUTE sequence was first applied to the brain of three healthy volunteers for ultrashort T2 contrast optimization. The following imaging parameters were used: field of view (FOV) = 24 cm, slice thickness = 5 mm, bandwidth (BW) = 125 kHz, flip angle = 70°, TR = 1000 ms, TE = 8 and 2200 μs (the second echo was acquired to assess the effectiveness of the long T2 white matter signal suppression), sampling points = 192, number of projections = 131, reconstruction matrix size = 256×256, single slice. The number of projections was undersampled to reduce the total scan time to 4.4 minutes. Six different TIs (280, 300, 320, 330, 340 and 360 ms) were used. The optimal TI was determined by measuring the signal to noise ratio (SNR) of the white matter on the 2nd echo image. This should be near zero since the ultrashort T2* components were expected to be decayed to zero or near zero, while the long T2 components in white matter were expected to be effectively inverted and nulled by the long adiabatic IR pulse.

To further investigate the signal source of the IR-dUTE images, T2* of the ultrashort T2* components as well as the rubber phantom were investigated using UTE and IR-dUTE acquisitions at different TIs. UTE images were acquired with 10 TEs (0.008, 0.2, 0.6, 1.5, 3, 5, 10, 15, 20, 30 ms) and a short TR of 100 ms with a scan time of 1 min for each image. IR-dUTE images were acquired with four TE combinations (TEs = 0.008/4.4, 0.2/4.4, 0.6/4.4, 1.5/4.4 ms). Other imaging parameters were similar to the contrast optimization study described previously. In addition, T2* measurement of the rubber phantom was separately performed using 2D non-slice selective UTE and IR-UTE acquisitions at four TEs (0.008, 0.2, 0.6, 1.5 ms). A 1-inch birdcage coil was used for signal excitation and reception. This approach was expected to provide an accurate measurement of T2* of the rubber phantom, facilitating evaluation of errors in T2* measurement with in vivo IR-dUTE imaging. Standard clinical sequences, including T1-weighted fast spin echo (FSE), T2-weighted FSE and proton-density (PD)-weighted FSE sequences were also performed for comparison.

The optimized and validated IR-dUTE sequence was then used to image each of the nine healthy volunteers for morphological mapping and quantitative evaluation of the ultrashort T2* components. IR-dUTE images of the brain together with a rubber phantom were acquired with four different TE combinations (TEs = 0.008/4.4, 0.2/4.4, 0.6/4.4 and 1.5/4.4 ms). Other imaging parameters were similar to these used in the contrast optimization study. The 2nd echo was fixed at 4.4 ms so that the subtracted IR-dUTE images could be used for high contrast morphological imaging as well as T2* and proton density quantification. RPD of the rubber phantom was quantified by comparing the UTE signal from rubber with that from water doped with ~24 mM MnCl2 (T2* ~ 400 μs).

Data Analysis

Quantitative evaluation of SNR, contrast to noise ratio (CNR) and T2* were performed on each volunteer. SNRs were calculated as the ratio of the mean signal intensity inside a user-drawn region of interest (ROI) to the standard deviation of the background noise. The SNR of the second echo image from the IR-dUTE sequence was calculated to specifically evaluate the effectiveness of the long T2 white matter signal suppression (a lower SNR means better suppression of the long T2 white matter signal). CNRs between the ultrashort T2* components and gray matter were calculated as their signal difference over the background noise. T2* values were obtained using a Levenberg-Marquardt fitting algorithm based on equation [1]. The analysis algorithm was written in Matlab (The Mathworks Inc. Natick, MA, USA) and was executed offline on the Dicom images obtained using the protocols described above. RPD was quantified based on equation [3].

Results

Figure 2 shows selected axial 2D IR-dUTE images of the ultrashort T2* components in white matter of the brain acquired at different TIs. Image contrast depends on the choice of TI. Significant residual signal from the long T2 components of white matter of the brain was observed at lower TIs (e.g., TI = 280 ms, TR = 1000 ms), as evidenced by the non-zero signal on the 2nd echo of the IR-dUTE image. This signal decreased with the increase of TI to around 340 ms, when near zero signal was observed for the white matter on the 2nd echo

image at a TE of 2.2 ms, suggesting excellent suppression of the long T2 components in white matter. Further increase in TI resulted in higher residual signal from the long T2 components in white matter. Although higher SNR and CNR were achieved for white matter at higher TIs, the IR-dUTE subtraction images were a mixture of signals from both short and long T2 components in white matter. Figure 3 shows SNR and CNR values as a function of TI, confirming an optimal TI of around 330 ms. As a result, a TR of 1000 ms and a TI of 330 ms were used in the subsequent studies.

Accuracy of the IR-dUTE sequence in measuring ultrashort T2* species is demonstrated in Figure 4. The rubber phantom has an ultrashort T2* of 0.34 ± 0.02 ms, when measured with both the non-slice selective 2D UTE and IR-UTE sequences. In vivo IR-dUTE imaging with a TI of 330 ms shows a T2* of 0.37 ± 0.09 ms for the rubber phantom, suggestion relatively accurate assessment of the short T2* species (with 9% overestimation). The ultrashort T2* components in white matter of the brain of the volunteer had a T2* of 0.47 ± 0.04 ms. This is slightly longer than that of the rubber phantom. When a TI of 360 ms was used a longer T2* of 4.16 ± 0.54 ms was observed, consistent with imperfect nulling of the long T2 components. The IR-dUTE signal is likely to be a mix of ultrashort T2* components and longer T2* components which are partly suppressed by the adiabatic IR pulse with a TI of 360 ms. The UTE signal mainly represents the long T2* components with minor contribution from the ultrashort T2* components. As a result, a much longer effective T2* of 15.5 ± 3.7 ms was observed with UTE data acquisitions for the same ROI.

Comparison between IR-dUTE imaging and clinical T1-FSE, T2-FSE and PD-FSE imaging of white matter of the brain was performed on another normal volunteer, as shown in Figure 5. Clinical FSE sequences with a TE of 10 ms or longer showed predominantly long signal from the long T2 components in white matter as well as those in gray matter and CSF. The IR-dUTE sequence showed near zero signal for the white matter on the 2nd echo with a TE of 2.2 ms. This directly confirmed that the long T2 components in white matter were efficiently suppressed by the adiabatic inversion pulse so that only the ultrashort T2* components were detected by the IR-dUTE first echo image. A RPD of 3.17 ± 0.28% was demonstrated for the ultrashort T2* components by comparing their signal intensities with that of the rubber phantom, which had a RPD of 35.2% as measured by the 3D UTE sequence.

Figure 6 shows echo subtracted IR-dUTE images of three healthy volunteers, as well as the corresponding T2* decay curves from selected ROIs. Single component exponential curve fitting showed mean T2* values between 0.33 to 0.55 ms, demonstrating that only the ultrashort T2* components were detected by the IR-dUTE sequences.

Table I shows detailed information including age, sex, T2* and RPD of each of the nine volunteers. The results demonstrate that the ultrashort T2* components in brain white matter have very short T2*s ranging from 0.32 ms to 0.59 ms and low RPDs ranging from 2.97% to 5.25%. On average, a mean SNR of 18.7 ± 3.7 and a mean CNR of 14.6 ± 2.4 between the ultrashort T2* white matter and gray matter were observed in 4.4 min scan time with a nominal voxel size of 1.25×1.25×5.0 mm^3. A short mean T2* of 0.42 ± 0.08 ms and low mean RPD of 4.05 ± 0.88% were demonstrated for the healthy volunteers at 3T.

Discussion

The IR-dUTE morphological imaging techniques consist of 1) a 2D UTE data acquisition scheme which employs a short half pulse excitation followed radial ramp sampling with a minimal nominal TE of 8 μs (Du J, et al, 2009); 2) a long adiabatic inversion recovery preparation pulse which provides robust inversion of long T2 components in white matter as well as long T2 components in gray matter, CSF and fat in the scalp and bone marrow (Waldman A, et al, 2003); 3) dual echo 2D UTE data acquisition which starts at a delay time appropriate for the inverted longitudinal magnetizations of long T2 components in white matter to reach the null point; 4) echo subtraction of the 2^{nd} echo image from the first one to suppress residual long T2 signal and provide selective imaging of the ultrashort T2* components in white matter. The quantitative IR-dUTE techniques consisted of IR-dUTE imaging at a series of TE delays to quantify T2* of the ultrashort T2* components in white matter of the brain using a NNLS exponential fitting algorithm (Du J, et al, 2010). The acquisition scheme can substantially diminish deviations of signal measurements from long T2 components in white matter, which have far higher signal than the ultrashort T2* components and may introduce significant errors if not effectively suppressed. The crucial parameter for the robustness of this technique is TI, which is related to TR and the T1 of the long T2 components in white matter (Du J, et al, 2010). Inappropriate choice of TI may leads to contamination from the long T2 components in white matter, thus producing overestimated T2* values. Whether an appropriate TI is chosen or not can be judged by measuring the residual white matter signal in the second echo image. In all our IR-dUTE images the white matter signal decayed to zero or near zero in the second echo with a TE of around 2 ms, confirming that an appropriate combination of TR and TI was used.

The existence of multiple water components in white matter is well recognized. Multi-component analysis of the Carr-Purcell-Meiboon-Gill (CPMG) T2 signal decay is one commonly used method to quantify myelin water (T2 ~ 10–50 ms), intra/extra axonal water (T2 ~ 80 ms) and interstitial water (T2 ~ 2000 ms) (MacKay A, et al., 2006; Moore GR, et al., 2000; Oh J, et al., 2006; Whittall KP, et al, 1997). The magnitude of the short T2 component is correlated well with the amount of myelin in rat sciatic nerve, indicating that multi-component T2 relaxation could be used to directly measure myelin in the peripheral nervous system. A three-pool model together with T2* analysis of multi-echo gradient echo data has been employed for in vivo multi-slice mapping of myelin water (T2* ~ 10 ms) content (Du YP, et al., 2007; Hwang D a 2008; Hwang D, et al., 2010). Nonexponential T2* decay was also identified in white matter by van Gelderen P et al. (van Gelderen P, et al., 2012). More recently a technique called direct visualization of short relaxation time component (ViSTa) has been developed to selectively image short T2* components (3 ms < T2* < 25 ms) (OH SJ, et al., 2013). In ViSTa two adiabatic inversion pulses are employed to invert and null the long T2 white and gray matter components, leaving the short T2* components to be detected with a conventional 2D gradient echo acquisition.

However, the literature regarding T1 relaxation in white matter is somewhat inconsistent. For example, Whittall et al. investigated the T1 distributions for 11 structures (five white matter and six gray matter) in brain using a saturation recovery approach, and found each of the structures was practically monoexponential, suggesting a single T1 component for both

white matter and gray matter (Whittall KP, et al., 1997). Several other groups have reported similar findings (Breger RK, et al., 1989; MacFall JR, et al., 1987). On the other hand, Does and Gore reported three components for both T1 and T2 relaxation in rat brain and trigeminal nerve in vivo (Does M, et al., 2002). The three-pool model is supported by Lancaster et al (Lancaster JL, et al., 2003). There are also several groups reporting two T1 components, with a shorter T1 for myelin water and a longer T1 for other longer T2 components in white matter (Koenig SH, et al., 1990; Stanisz GJ, et al., 1999). In this study, we assumed a single T1 component for the longer T2 components which are inverted and nulled by the single adiabatic inversion pulse with an appropriate TI. The results in Figure 4 suggest that this assumption is reasonable since the longer T2* components were well suppressed and signal detected by the IR-dUTE sequence with a TR of 1000 ms and a TI of 330 ms could be modeled with a single ultrashort T2* component.

T2* values from IR-dUTE imaging are broadly consistent with values published in literature. Nayak et al. first employed a long T2 saturated ultrashort echo time (UTE) sequence to directly evaluate the ultrashort T2* components in white matter of a fixed cadaveric brain using a whole body clinical scanner, and found T2* values ranged from 100 to 350 μs (Nayak KS, et al., 2000). Erean et al employed a bi-component approach to evaluate 3D UTE T2* signal and found a mean T2* of 0.26 ms for the ultrashort T2 component in white matter, and 0.38 ms for the ultrashort T2 component in gray matter (Ercan E, et al., 2012). These approaches are sensitive to SNR limitation and/or lack of image contrast for the ultrashort T2* components in white matter. Waldman et al. first introduced adiabatic inversion recovery prepared UTE imaging of the ultrashort T2* components in white matter of the brain in vivo using a whole body clinical 1.5 T scanner (Waldman A, et al., 2003). The use of adiabatic IR preparation pulse allows efficient suppression of long T2 components, leaving excellent image contrast for the ultrashort T2 components in white matter.

Direct imaging of myelin could improve specificity in evaluating myelination and demyelination. The NMR spectral properties of myelin have been studied by several groups. Lecar et al. investigated anhydrous preparations of myelin by broad-line proton spectroscopy and concluded that myelin water is in a liquid-crystalline state (Lecar H, et al., 1971). Ramani et al. studied fixed human white matter samples using multi-component fitting of spin-echo decays and found T2 values of ~50 μs for myelin protons (Ramani A, et al., 2003). Horch et al. studied the origins of the ultrashort T2 proton NMR signals in myelinated nerve, and found the ultrashort T2 signals (50 μs < T2 < 1 ms) could be potentially used a specific measure of myelin content (Horch RA, et al., 2011). More recently, Wilheml et al. investigated the spectrum of myelin in the spinal cord and found that the spectrum could be modeled as a sum of super-Lorentizians with a T2* distribution covering a wide range of values from 8 μs to 26 ms (Wilhelm MJ, et al., 2012). They concluded that the ultrashort T2* signal of rat and bovine spinal cord samples came predominantly from myelin lipids (Wilhelm MJ, et al., 2012).

The histological correspondence of the IR-dUTE signal in white matter remains to be determined. However, the ultrashort T2* components assessed by the IR-dUTE technique are unlikely to solely correspond to myelin water from the T2 or T2* multi-component

analysis techniques referenced previously since our T2*s are more than 20 times shorter. Proton densities of the ultrashort T2* components are around 3–5%, which is far lower than the myelin water fractions reported in the literature, e.g., 15% (Koenig SH, et al., 1990), 32% (Stanisz GJ, et al., 1999), 19% (Does MD, et al., 2002), 17% (Lancaster JL, et al., 2003), and 10% (Du YP, et al., 2007). This large difference further suggests that the signal source for IR-dUTE imaging is unlikely to be solely myelin water. The IR-dUTE signal source may also be different from that found in the above NMR spectroscopic studies since our T2* values are about 5 to 10 times longer. We suspect that the IR-dUTE signal source may include both myelin and water tightly bound to myelin. Another explanation might arise from the fact that whole body clinical scanner used in this study has lower RF and gradient system performance and is therefore incapable of detecting the very short T2* components in white matter of the brain when compared with high performance NMR spectrometers. It is likely that part of myelin water (i.e., water tightly bound to macromolecular structures in white matter) and protons in phospholipids within cell membranes both contribute to the IR-dUTE signal. Further work is needed to identify the signal source for IR-dUTE imaging using clinical whole body scanners, and to establish the link between the IR-dUTE signal and macromolecular content.

There are several limitations of this study. Firstly, only healthy volunteers were recruited. Future work will include patients with multiple sclerosis. Secondly, the IR-dUTE sequence was based on 2D radial ramp sampling, and is subject to artifacts from eddy currents, field homogeneity and gradient nonlinearity. Gradient profile distortion may result in an imperfect slice profile and out-of-slice signal contamination. Correction of the slice-select gradients and time-varying main field $B_0(t)$ caused by eddy currents are helpful in reducing out-of-slice signal contamination (Lu A, et al., 2008). Thirdly, the IR-dUTE sequence is relatively time inefficient since it requires summation of two acquisitions with reversed slice selection gradient polarities to form a conventional slice profile. Undersampled projection acquisitions were used to reduce the total scan time at the cost of streak artifacts and reduced SNR (Du J, et al., 2011). Fourthly, T1 was not measured in our study, but taken from literature (Nayak KS, et al., 2000). In Nayak's study a long T2 suppression pulse was followed by a crusher gradient to suppress the long T2 components in white matter of the brain. This approach is sensitive to B1 inhomogeneity as well as long T2 signal recovery during the dead time (i.e. the time between the end of the 90° pulse and the peak of the RF excitation pulse). More accurate T1 measurements may be achieved with IR-dUTE based approaches, e.g., variable flip angle and/or different TR/TI combinations. Further investigation is required in this area. Fifthly, the origin of the IR-dUTE signal requires further investigation. D2O-H2O exchange studies of brain white matter samples using the IR-dUTE sequence on a whole body scanner may further our understanding on the relative contributions of myelin water protons and non-water protons to the IR-dUTE signal, and will be performed in future studies. Sixthly, only a single slice was imaged and quantified. Multi-slice IR-dUTE sequences can be implemented by employing a slice selective adiabatic IR pulse followed by 2D UTE dual echo acquisition (Du J, et al., 2008), or 3D IR-dUTE acquisition (Du J, et al., 2011).

In summary, we have demonstrated the feasibility of selective imaging and quantitative evaluating the T2*s and RPDs of the ultrashort T2* components in white matter of the brain

in vivo using a whole body clinical 3T scanner. A short T2* of around 0.42 ± 0.08 ms, and a low RPD of 4.05 ± 0.88% were found for the ultrashort T2* components in white matter of the brain of healthy volunteers at 3T. The signal source is likely to be from protons in cell membranes as well as water tightly bound to macromolecular structures in white matter. Demonstration of high contrast morphological imaging of the ultrashort T2* components in white matter together with quantitative measurement of their MR relaxation times (e.g., T2* and T1) and tissue properties (e.g., proton density) may significantly advance the study of white matter disease.

Acknowledgments

The authors thank grants support from GE Healthcare and 1R21 AR063894-01A1.

References

1. Breger RK, Rimm AA, Fischer ME, Papke RA, Haughton VM. T1 and T2 measurements on a 1. 5 T commercial MR imager. Radiology. 1989; 171:273–276. [PubMed: 2928538]
2. Biswas R, Bae CW, Diaz E, Masuda K, Chung CB, Bydder GM, Du J. Ultrashort echo time (UTE) imaging with bi-component analysis: bound and free water evaluation of bovine cortical bone subject to sequential drying. Bone. 2012; 50:749–755. [PubMed: 22178540]
3. Does MD, Gore JC. Compartmental study of T1 and T2 in rat brain and trigeminal nerve in vivo. Magn Reson Med. 2002; 47:274–283. [PubMed: 11810670]
4. Du J, Bydder M, Takahashi AM, Carl M, Chung CB, Bydder GM. Short T2 contrast with three-dimensional ultrashort echo time imaging. Magn Reson Imaging. 2011; 29:470–82. [PubMed: 21440400]
5. Du J, Carl M, Bydder M, Takahashi A, Chung CB, Bydder GM. Qualitative and quantitative ultrashort echo time (UTE) imaging of cortical bone. J Magn Reson. 2010; 207:304–311. [PubMed: 20980179]
6. Du J, Hamilton G, Takahashi AM, Bydder M, Chung CB. Ultrashort TE spectroscopic imaging (UTESI) of cortical bone. Magn Reson Med. 2007; 5:1001–1009. [PubMed: 17969110]
7. Du J, Takahashi AM, Bydder M, Chung CB, Bydder GM. Ultrashort TE imaging with off-resonance saturation contrast (UTE-OSC). Magn Reson Med. 2009; 62:527–531. [PubMed: 19449436]
8. Du J, Takahashi A, Bydder M, Chung CB. Two dimensional ultrashort echo time imaging using a spiral trajectory. Magn Reson Imaging. 2008; 26:304–312. [PubMed: 18096346]
9. Du YP, Chu R, Hwang D, Brown MS, Kleinschmidt-DeMasters BK, Singel D, Simon JH. Fast multislice mapping of the myelin water fraction using multicompartment analysis of T2* decay at 3T: a preliminary postmortem study. Magn Reson Med. 2007; 58:865–870. [PubMed: 17969125]
10. Ercan, E.; Bornert, P.; Webb, A.; Ronen, I. Whole-brain tissue-based assessment of the ultrashort T2 component using 3D UTE MRI relaxometry. Proceedings of the 20th Annual Meeting of ISMRM; Melbourne, Australia. 2012. p. 4279
11. Henkelman RM, Stanisz GJ, Graham SJ. Magnetization transfer in MRI: a review. NMR Biomed. 2001; 14:57–64. [PubMed: 11320533]
12. Horch RA, Gore JC, Does MD. Origins of the ultrashort T2 1H NMR signals in myelinated nerve: a direct measure of myelin content? Magn Reson Med. 2011; 66:24–31. [PubMed: 21574183]
13. Hwang D, Du YP. Improved myelin water quantification using spatially regularized non-selective least square algorithm. J Magn Reson Imaging. 2009; 30:203–208. [PubMed: 19557738]
14. Hwang D, Kim DH, Du YP. In vivo multi-slice mapping of myelin water content using T2* decay. NeuroImage. 2010; 52:198–204. [PubMed: 20398770]
15. Koenig SH, Brown RD, Spiller M, Lundborn N. Relaxometry of brain: why white matter appears bright in MRI. Magn Reson Med. 1990; 14:482–495. [PubMed: 2355830]
16. Lancaster JL, Andrews T, Hardies LJ, Dodd S, Fox PT. Three-pool model of white matter. J Magn Reson Imaging. 2003; 17:1–10. [PubMed: 12500269]

17. Larson PE, Conolly SM, Pauly JM, Nishimura DG. Using adiabatic inversion pulses for long-T2 suppression in ultrashort echo time (UTE) imaging. Magn Reson Med. 2007; 58:952–961. [PubMed: 17969119]
18. Lecar H, Ehrenstein G, Stillman I. Detection of molecular motion in lyophilized myelin by nuclear magnetic resonance. Biophys J. 1971; 11:140–145. [PubMed: 5100752]
19. Lu A, Daniel BL, Pauly JM, Pauly KB. Improved slice selection for R2* mapping during cryoablation with eddy current compensation. J Magn Reson Imaging. 2008; 28:190–198. [PubMed: 18581340]
20. MacFall JR, Wehrli FW, Breger RK, Johnson CA. Methodology for the measurement and analysis of relaxation times in proton imaging. Magn Reson Imaging. 1987; 5:209–220. [PubMed: 3041152]
21. MacKay A, Laule C, Vavasour I, Bjarnason T, Kolind S, Madler B. Insights into brain microstructure from the T2 distribution. Magn Reson Imaging. 2006; 24:515–525. [PubMed: 16677958]
22. Moore GR, Leung E, McKay AL, Vavasour IM, Whittall KP, Cover KS, Li DK, Hashimoto SA, Oqer J, Sprinkle TJ, Paty DW. A pathology-MRI study of the short-T2 component in formalin-fixed multiple sclerosis brain. Neurology. 2000; 55:1506–1510. [PubMed: 11094105]
23. Nayak, KS.; Pauly, JM.; Gold, GE.; Nishimura, DG. Imaging ultrashort T2 species in the brain. Proceedings of the 8th Annual Meeting of ISMRM; Denver, USA. 2000. p. 509
24. Oh J, Han ET, Pelletier D, Nelson SJ. Measurement of in vivo multi-component T2 relaxation times for brain tissue using multi-slice T2 prep at 1. 5 and 3 T. Magn Reson Imaging. 2006; 24:33–43. [PubMed: 16410176]
25. Oh SJ, Bilello M, Schindler M, Markowitz CE, Detre JA, Lee J. Direct visualization of short transverse relaxation time component (ViSTa). NeuroImage. 2013 (in press).
26. Ramani A, Aliev AE, Barker GJ, Tofts PS. Another approach to protons with constricted mobility in white matter: pilot studies using wideline and high-resolution NMR spectroscopy. Magn Reson Imaging. 2003; 21:1039–1043. [PubMed: 14684209]
27. Ramani A, Dalton C, Miller DH, Tofts PS, Barker GJ. Precise estimation of fundamental in-vivo MT parameters in human brain in clinically feasible times. Magn Reson Imaging. 2002; 20:721–731. [PubMed: 12591568]
28. Stanisz GJ, Kecojevic A, Bronskill MJ, Henkelman RM. Characterizing white matter with magnetization transfer and T2. Magn Reson Med. 1999; 42:1128–1136. [PubMed: 10571935]
29. Techawiboonwong A, Song HK, Leonard MB, Wehrli FW. Cortial bone water: in vivo quantification with ultrashort echo-time MR imaging. Radiology. 2008; 248:824–833. [PubMed: 18632530]
30. van der Knaap, MS.; Valk, J. Magnetic resonance of myelination and myelin disorders. Heilmann, U.; Mennecke-Buhler, D., editors. Springer; Berlin: 2005. p. 1-19.
31. van Gelderen P, de Zwart JA, Lee J, Sati P, Reich DS, Duyn JH. Nonexponential T2* decay in white matter. Magn Reson Med. 2012; 67:110–117. [PubMed: 21630352]
32. Waldman A, Rees JH, Brock CS, Robson MD, Gatehouse PD, Bydder GM. MRI of the brain with ultra-short echo time pulse sequences. Neuroradiology. 2003; 45:887–892. [PubMed: 14508620]
33. Whittall KP, MacKay AL. Quantitative interpretation of NMR relaxation data. J Magn Reson. 1989; 84:134–152.
34. Whittall KP, MacKay AL, Graeb DA, Nugent RA, Li D, Paty DW. In vivo measurement of T2 distributions and water contents in normal human brain. Magn Reson Med. 1997; 37:34–43. [PubMed: 8978630]
35. Wilhelm MJ, Ong HH, Wehrli SL, Li C, Tsai PH, Hackney DB, Wehrli FW. Direct magnetic resonance detection of myelin and prospects for quantitative imaging of myelin density. Proc Natl Acad Sci USA. 2012; 109:9605–9610. [PubMed: 22628562]
36. Wolff SD, Balaban RS. Magnetization transfer contrast (MTC) and tissue water proton relaxation in vivo. Magn Reson Med. 1989; 10:135–144. [PubMed: 2547135]

Highlights

- MRI of the ultrashort T2* components in white natter of the brain is investigated.
- The ultrashort T2* components are detected with a 2D UTE sequence using a clinical 3T scanner.
- The contrast mechanism relies on effective suppression of the long T2 components.
- The IR-dUTE technique provides robust measurement of T2* and proton density of the ultrashort T2* components.

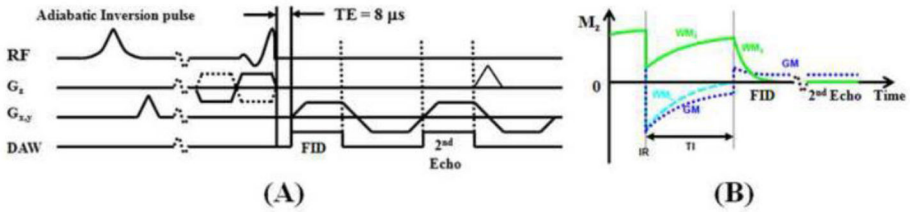

Figure 1.

Pulse sequence for 2D UTE imaging using half pulse excitation and radial ramp sampling with a minimal nominal TE of 8 μs (A). An adiabatic inversion recovery preparation pulse together with dual echo acquisition was used to create short T2 contrast (B). The adiabatic IR pulse provides robust inversion of the longitudinal magnetizations of gray matter (GM) and the long T2 components in white matter (WM_L). The ultrashort T2 components in white matter (WM_S) experience significant transverse relaxation during the long adiabatic inversion process, and are not inverted but partly saturated. The UTE acquisition starts when the inverted longitudinal magnetization of WM_L reaches the null point, leaving signals from WM_S and residual GM to be detected by the FID acquisition. The 2^{nd} echo contains signal from GM, with near zero signal from WM_S due to its short T2*. Subtraction of the 2^{nd} echo from the FID provides selective imaging of WM_S.

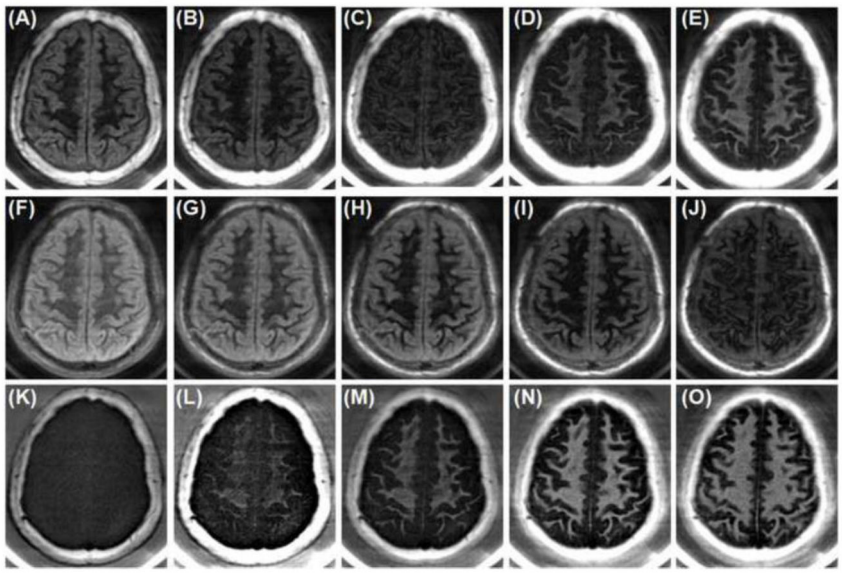

Figure 2.

IR-dUTE imaging of the ultrashort T2* components in white matter of the brain of a 34 year old healthy volunteer with a TR of 1000 ms and TI of 280 ms (A, F, K), 300 ms (B, G, L), 320 ms (C, H, M), 340 ms (D, I, N) and 360 ms (E, J, O). The 1st echo UTE images with a TE of 8 μs are shown in the 1st row (A–E). The 2nd echo UTE images with a TE of 2.2 ms are shown in the 2nd row (F–J). The corresponding echo subtraction images are shown in the 3rd row (K–O).

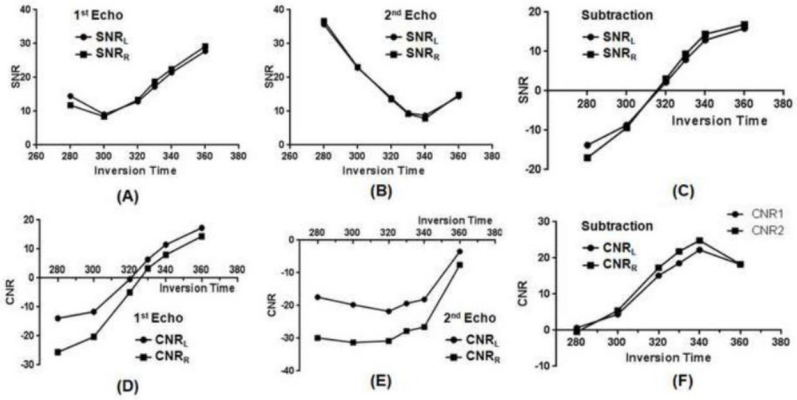

Figure 3.

SNR of the white matter for the 1st echo (A), 2nd echo (B) and echo subtraction images (C), as well as the CNR of the white matter for the 1st echo (D), 2nd echo (E) and echo subtraction images (F). Minimal SNR for the white matter was achieved with a TI of around 330 ms, which is the TI corresponding to virtually complete nulling of the long T2 components in white matter. SNR and CNR for both the right and left side of the brain were measured.

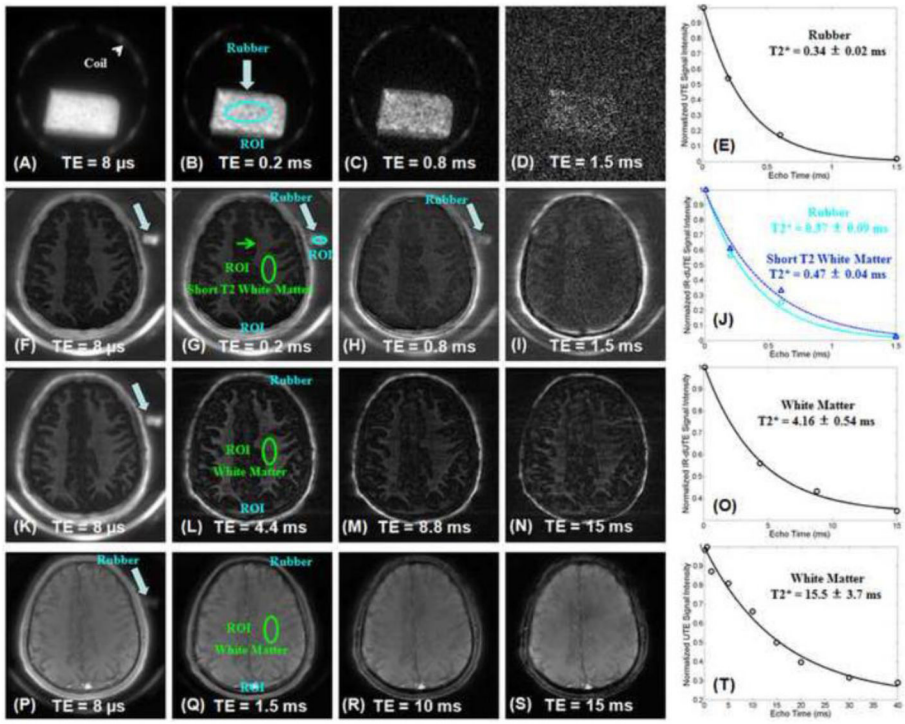

Figure 4.

2D non-slice selective UTE images of the rubber phantom with TEs of 8 μs (A), 0.2 ms (B), 0.6 ms (C) and 1.5 ms (D). Single component fitting shows a T2* of 0.34 ± 0.02 ms for the rubber phantom (E). IR-dUTE subtraction images of a healthy volunteer with a TR of 1000 ms, TI of 330 ms and TEs of 8 μs (F), 0.2 ms (G), 0.6 ms (H) and 1.5 ms (I). Single component fitting shows a T2* of 0.37 ± 0.09 ms for the rubber phantom and a T2* of 0.47 ± 0.04 ms for the ultrashort T2* components in white matter of the brain (J). IR-dUTE images of the same volunteer with a TR of 1000 ms, TI of 360 ms and TEs of 8 μs (K), 4.4 ms (L), 8.8 ms (M) and 15 ms (N). Single component fitting shows a T2* of 4.16 ± 0.54 ms for the same ROI, suggesting longer T2* components contribute to the IR-dUTE signal. Regular UTE imaging of the same volunteer with a TR of 100 ms and TEs of 8 μs (K), 1.5 ms (L), 10 ms (M) and 15 ms (N). Single component fitting shows a T2* of 15.5 ± 3.7 ms for the same ROI, suggesting long T2 components dominate the UTE signal.

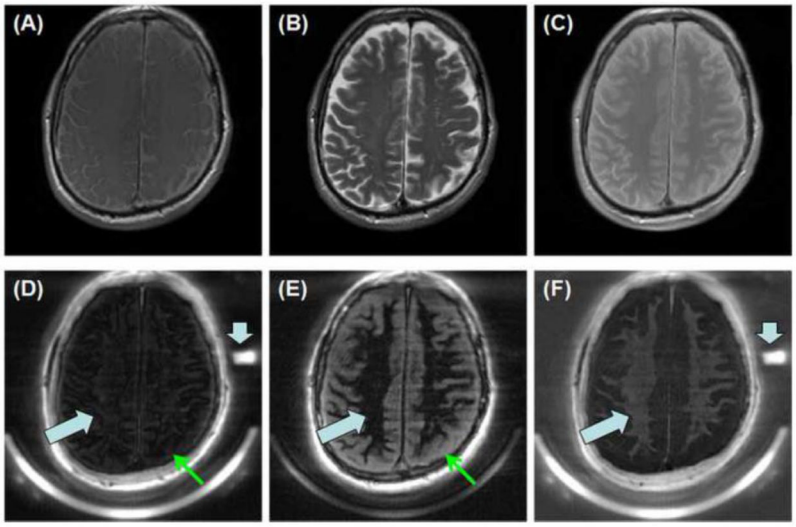

Figure 5.

T1-FSE (A), T2-FSE (B), PD-FSE (C) as well as IR-dUTE imaging of the ultrashort T2 components in white matter of the brain of a healthy volunteer (D–F). Dual echo images were acquired with TEs of 8 μs (D) and 4.4 ms (E). The later echo image was subtracted from the first one to selectively depict short T2* components in white matter (F). Signals from the long T2 component in white matter were nulled by the adiabatic inversion pulse (thick arrows). Signals from the long T2 gray matter were suppressed through subtraction (thin arrows), leaving signal from tightly bound myelin water to be selectively depicted (F). A low RPD of 3.17 ± 0.28% was demonstrated for the ultrashort T2* components by comparing their signal intensities with that of the rubber phantom (short thick arrows).

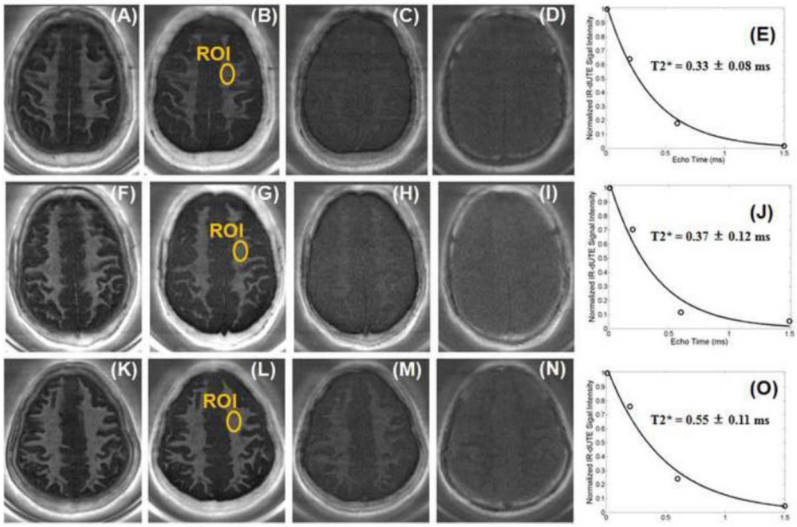

Figure 6.

IR-dUTE imaging of the ultrashort T2 components in white matter of three healthy volunteers, 37 years old (1st row), 63 years old (2nd row) and 40 years old (3rd row) with TEs of 8 μs (A, F, K), 0.2 ms (B, G, L), 0.6 ms (C, H, M) and 1.5 ms (D, I, N) as well as the corresponding single component T2* fitting (E, J, O). Short T2*s of 0.33 ms, 0.37 ms and 0.55 ms were demonstrated, respectively.

Table I

Age, sex, and mean T2*s and RPD of the ultrashort T2* components in white matter of the brain of nine healthy volunteers.

volunteers	age	sex	T2* [ms]	Relative PD [%]
1	69	male	0.44 ± 0.08	3.17 ± 0.28
2	63	male	0.37 ± 0.09	3.37 ± 0.35
3	62	male	0.39 ± 0.08	4.35 ± 0.38
4	60	male	0.47 ± 0.04	4.26 ± 0.49
5	48	male	0.32 ± 0.09	3.24 ± 0.42
6	40	male	0.59 ± 0.03	2.97 ± 0.21
7	37	male	0.35 ± 0.06	5.06 ± 0.43
8	34	male	0.39 ± 0.06	5.25 ± 0.34
9	34	male	0.36 ± 0.05	4.81 ± 0.37
Average	50 ± 14	-	0.42 ± 0.08	4.05 ± 0.88